20th Australasian Fluid Mechanics Conference
Perth, Australia
5-8 December 2016

Pair-Particle Separation Statistics of Drifters in Tidal Shallow Water

K.A. Suara[1], R.J. Brown[1], H. Chanson[2] and M. Borgas[3]

[1]Science and Engineering Faculty, Queensland University of Technology, Queensland 4000, Australia

[2]School of Civil Engineering, The University of Queensland, Queensland 4072, Australia

[3] Marine and Atmospheric Research
Commonwealth Scientific and Industrial Research Organisation (CSIRO), Aspendale, VIC 3195, Australia

Abstract

In estuaries and natural water channels, the estimate of turbulent diffusivity is important to the modelling of scalar transport and mixing. Data from multiple deployments of low and high resolution clusters of GPS-drifters are used to examine dispersive behaviour of a small tidal estuary. Relative dispersion from pair-particle separation and finite scale Lyapunov exponents (FSLEs) are employed. Relative dispersion within the natural channel indicates weaker than Richardson's power law exponent in the range of 1 – 2. The FLSE scales as $\lambda \sim \delta^{-2/3}$ in a small spatial scale range of $\delta \sim 2 - 10$ m. The FSLE analysis suggests the presence of exponential dispersive behaviour, i.e. chaotic mixing at medium to large spatial scales. The results provide insights into accurately parameterizing unresolved mixing processes in typical tidal shallow bounded estuary.

Introduction

Relative dispersion in a fluid is a fundamental area of study that dates back to Richardson [1]. An extensive review of the statistical frameworks is compiled in [2, 3]. Richardson's power law relationship between relative dispersion, D_p, and elapsed time, t, implies $D_p^2 \sim \varepsilon t^{\alpha}$ with $\alpha = 3$. Both this relationship and the relative diffusivity, $K_p \sim d^{\gamma}$ with $\gamma = 4/3$, are found to be related to the Kolmogorov's energy cascade law $E(k) \sim \varepsilon^{2/3} k^{-5/3}$, where ε is the TKE dissipation rate, d is the length scale and k is the wave number, in three-dimensional homogeneous flow in isotropic turbulence within the inertial range [4, 5]. Many environmental flows are two-dimensional, dominated by inhomogeneity and anisotropy, which leaves the question on the applicability of such relationships. Richardson-like relationships were observed in the subsurface flow in the North Atlantic, with a power $\gamma = 2.2$ at time, $t > 10$ days and length scale, $l > 50$ km [6]. Spydell et al. [7] observed a Richardson-like power law relationship with $\gamma = 3/2$ and $\alpha = 2/3$ with time, $t \leq 600$ s and length scale range of 5 – 50 m in a surf zone with breaking waves. Brown et al. [8] observed a power law relationship with $\gamma = 4/3$ and $\alpha = 1/5$ with time, $t \leq 100$ s and length scale range of 1 – 10 m in a rip channel with the dispersion dominated by horizontal shear. The range of these observations indicates a clear deviation from existing theory due to the combination of underlying physical processes. Interestingly, no other literature to date experimentally examined the relative dispersion of passive particles in shallow tidal estuaries. The paper examines the dispersion regimes in tidal shallow estuaries at time scale less than a tidal period and length scale ranging from 0.1 to few metres using deployments of high resolution (HR) and low resolution (LR) Lagrangian drifters.

Field, instrumentation and experiment

A series of field studies were conducted at Eprapah Creek (Longitude 153.30º East, Latitude -27.567º South), a sub-tropical shallow tidal estuary, discharging into Moreton Bay, Eastern Australia. The estuarine zone extends to 3.8 km inland and is well sheltered from wind by mangroves [9]. The lowest bed elevation along the mid-estuary was about 2.5 m below Mean Sea level (MSL), as surveyed on 30/07/2015. The channel width was limited to 60 m at high tide and 25 m at low tide. The drifter datasets analysed herein, are from two separate field experiments.

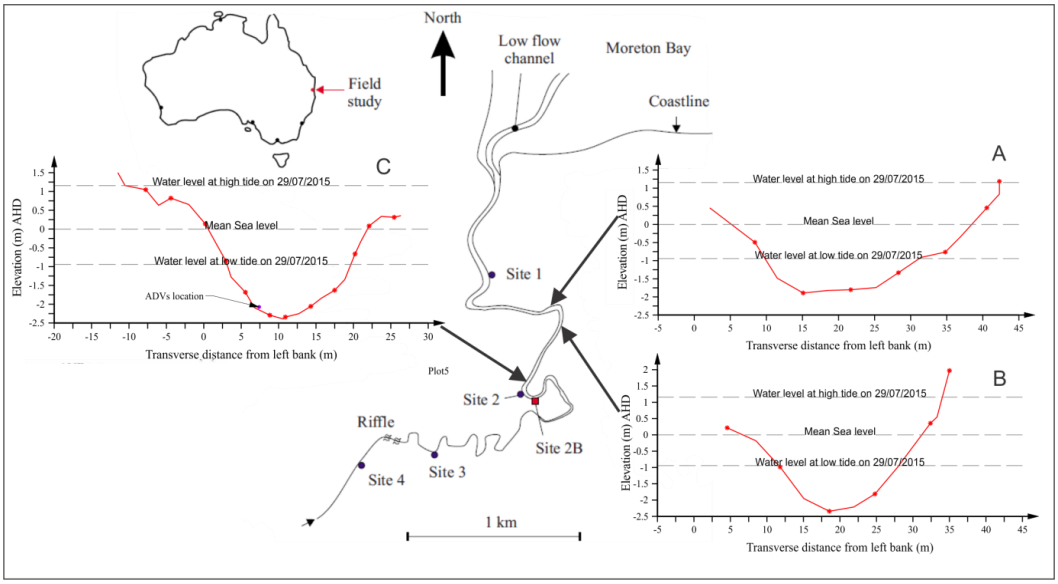

Figure 1. Eprapah Creek estuarine zone, including surveyed sampling cross section on 30 July 2015.

The first experiment (EM14) was carried out on 22 May 2014 during an incoming neap tide. A cluster of three HR and five LR drifters were deployed from the river mouth and were allowed to drift for up to 4.5 hours (2.2 km inland). The second experiment was carried out in between 29 – 31 July 2015 in multiple deployments during two sequential flood tides using four HR and 18 LR drifters. Drifter deployments were made within the straight test section between adopted mean thread distance (AMTD) 1.60 – 2.05 km, i.e. between cross sections B and C (Figure 1). The length of deployment varied between 81 and 3961 s. A range of tide, wind and flow conditions were encountered during the field studies. Eprapah Creek is characterised by semi-diurnal tides and a diurnal wind pattern. The average wind speed varied between 0 – 4 m/s mostly aligned in the streamwise direction during the day and the night and wind speed varied between 0 – 1 m/s without a directional preference. Table 1 summarises the field conditions. Note that all deployments were conducted during the flood tide.

Exp.	Tidal range (m)	Average Wind speed (m/s)	Duration of exp.	Deployment coverage (AMTD)	Deployment type
EM14	1.4 (Neap, flood)	< 1.1	4.5 hours	0 – 2.2 km	Single deployment
EJ15	2.03 (Neap, flood)	0.65	3.02 hours	1.60 – 2.05 km	Repeated deployments

Table 1. Overview of the experimental condition for the field studies

The HR drifters, equipped with differential RTK-GPS integrated receiver, were sampled at 10 Hz with a position accuracy ~2 cm [10]. The LR drifters contained off-the-shelf Holux GPS data loggers with absolute position accuracy, between 2 – 3 m, and were sampled at 1 Hz. The drifters were positively buoyant for continuous satellite position fixation with unsubmerged height < 3 cm in order to limit the direct wind effect [10]. The drifter data yielded surface velocities that compared well with acoustic Doppler current profiler (ADCP) surface horizontal velocity measurements ($R^2 > 0.9$).

Data analysis

Quality Control

The quality of drifter datasets were controlled using velocity and acceleration thresholding procedure [9, 10]. Flagged data were replaced with linearly interpolated points using data at valid end points, where the gap was less than 20 s. The drifter data were transformed into channel-based streamwise (s), cross stream (n), up (u) coordinate system based coordinate [10]. For the HR drifters, the position time series was further treated with a low-pass filter of cut-off frequency, F_c = 1 Hz and subsampled to intervals of 1 s to remove the instrument noise at high frequencies [10]. Figure 2 shows the sample trajectories from the drifter experiments (EM14 & EJ15) coloured in terms of the mean horizontal velocity.

Relative dispersion

The relative dispersion is closely tied with scalar mixing processes, compared to single particle dispersion. A common measure to describe dispersion in this frame is the mean square separation of pair particles, D_p^2 defined as:

$$D_{pi}^2(t,r_o) = \left\langle (r_i(t) - r_{oi})^2 \right\rangle - \left\langle (r_i(t) - r_{oi}) \right\rangle^2, \qquad (1)$$

where i represents 's' and 'n' directions, < > denotes ensemble average over all available pair realisations at time, t and r_o is the initial separation of a pair. The slope of the relationship $D_p^2(t)$ against t, changes with time and indicates the dispersion regimes responsible for the particle separation in a turbulent flow field [3]. Four distinctive regimes may be described as follow:

1. $D_p^2 \sim t$ diffusive regime, diffusivity is constant;
2. $D_p^2 \sim t^2$ "Ballistic" dispersion regime;
3. $D_p^2 \sim t^3$ Richardson's power law regime; and
4. $D_p^2 \sim exp(t)$ exponential separation regime.

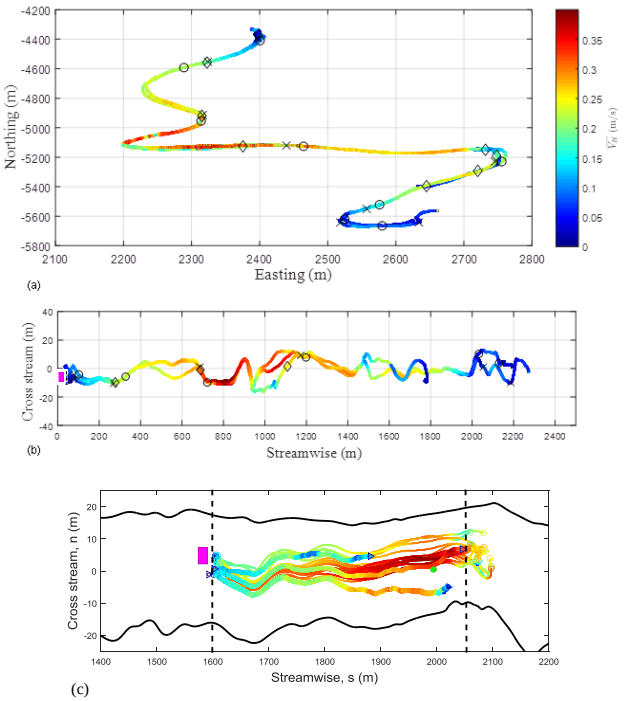

Figure 2. Sample drifter trajectories coloured by the mean horizontal velocity V_H (m/s). (a) e-n-u coordinate of HR drifters deployed from May 2014 (EM14) deployments; (b) s-n-u coordinate of HR drifters during May 2014 (EM14) deployment; (c) s-n-u cordinates of LR amd HR drifters clusters (single deployment) from July 2015 (EJ15) deployments. Pink box indicates the deployment point. Note the difference in the scale x-axis scale for the experiments. [e-n-u is interpreted as east –north up)

The effect of initial separation on D_p^2 and diffusivity K_p estimates were tested in terms of bins of r_o between 0 – 2 m, 2 – 8 m, 8 – 16 m and > 16 m. Focusing on the bulk of original pairs, the analysis is considered only up to an elapsed time t = 1000 s. Assuming that the flow field was stationary and that all drifters were subjected to the same motion during each experiment, the number of realisations per clusters were further increased by considering overlapped pair-particle segments [8]. Pair particles were restarted after 50 s, i.e. greater than twice the integral time scale T_L~ 20 s, to allow de-correlation of particle motions [9]. For example, an original pair particle data set of 2000 s duration would result in realisations between 0 – 1000 s, 50 – 1050 s, 100 – 1100 s etc., creating 20 additional realisations (not independent). This overlapping procedure reduced the variance of $D_p^2(t)$ without distorting its overall slope when compared with zero overlapping estimate.

Finite Scale Lyapunov Exponents

The finite scale Lyapunov exponent (FSLE) is an alternative approach to examine pair particle separation [11]. The dispersion is quantified by the ensemble-averaged time that the pair-particle separation grows from a distance δ_n to δ_{n+1}. FLSE is an inverse temporal scale, λ and varies as a function of spatial scale δ such that:

$$\lambda(\delta) = \frac{ln(\eta)}{\langle \Delta t_n \rangle}, \qquad (2)$$

where $\Delta t_n = t_{n+1} - t_n$ is the time taken for particle separation to grow from δ_n to $\eta\delta_n$, η >1 is the parameter that controls the finite scales over which the calculations are made and angle bracket

indicates ensemble averaging. The slope of $\lambda(\delta)$ curve can be related to different dispersion regimes in corresponding relative dispersion estimates. The regimes are characterised by the power law exponent a in the relation $\lambda(\delta) \propto \delta^a$ and are described in terms of their spatial scale relative to the size of energy containing eddies, L as follows:

1. For $\lambda(\delta) \approx \lambda_o$, a constant temporal scale occurs with spatial scale $\delta << L$. This regime corresponds to an exponential growth in $D_p^2(t)$ and separation are associated with chaotic advection.
2. $-2 < a < 0$ for $\delta \geq L$ indicating inertial subrange. Within this range, Richardson's Law behaviour corresponds to a power, a = -2/3 based on the dimensional arguments in [11] a = -1 correspond to a "Ballistic" regime.
3. $-2 \geq a$ for $\delta >> L$; where a power of -2 corresponds to a diffusive regime and steeper slopes associated sub-diffusive behaviour [11].

$\lambda(\delta)$ is sensitive to the choice of η and the smallest value that provides consistent estimate with coarser parameters is recommended [11].

Figure 3 shows the effect of η on the λ for different values of η. η = 1.05 producing results not significantly deviated from those obtained with η > 1.05 while η = 1.01 resulted in a clear shift in the FSLE curve. Hence, η = 1.05 is employed herein. Convergence of particle pair led to particle often recrossing δ_n and δ_{n+1}. For a paired-particle realisation, all particle possible crossings between δ_n and δ_{n+1} are included in the calculation of $<\Delta t_n>$ using fastest crossing principle [11]. Therefore, a pair-particle realisation could contribute to more than one value of Δt_n and significantly increased the number of degree of freedom (DOF) of the FSLE calculation. λ estimate with less than five number realisations are not included.

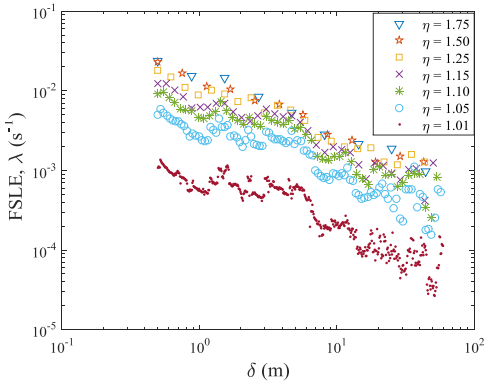

Figure 3. Sensitivity analysis of FSLE to finite scale parameter, η.

Results and discussions

Effect of initial separation distance

Figure 4 shows the relative dispersion as a function of time, for different initial separation distance. Note that D_p reflects the spatio-temporal growth of a patch because the original separation, r_o, is removed from D_p. In general, the particles travelled along similar streamlines subject to some underlying small-scale turbulence. At large separations, the particles experienced dispersion induced by shear and larger-scale fluctuations. For all initial separation, streamwise relative dispersion grew with power between 1.5 and 2. The side boundary suppressed spreading in the cross stream, reducing the growth of dispersion close to a power of 1, within an elapsed time of 30 s. With the exception of the large initial separation (r_o > 16 m), the diffusivity values exhibited no discernible dependence on the initial separation, r_o (not shown). The diffusivity exhibited dependence on a separation length scale not significantly deviated from Richardson's 4/3 power law. Because of the different behaviour for the pair-particles with r_o > 16 m, only particles with r_o < 16 m are included in the estimates of D_p^2.

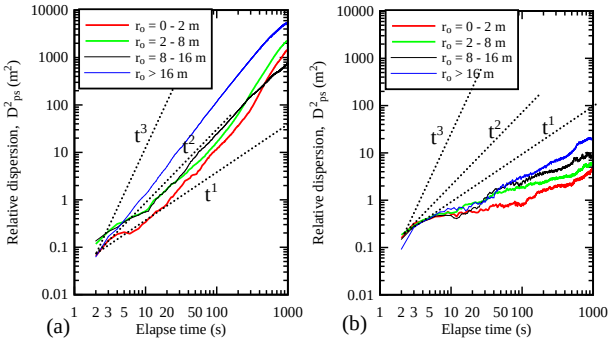

Figure 4. Dispersion as a function of elapsed time, t (a) Streamwise (b) Cross-stream directions; Black slant-dashed lines correspond to power law relationship

Observed dispersion regimes

Figure 5 shows the plots of relative dispersion, $D_p^2(t)$ and the FSLE , $\lambda(\delta)$ for cluster of HR and LR drifters deployed during EM14 field experiment. The difference between the curves for datasets from the HR and LR drifters could be related to difference in their position uncertainty [12] and physical dimensions [10]. Both datasets revealed a growth of D_p^2 with time to the power 2 in the first 20 s and slowed down at longer times. Spreading in the cross stream was suppressed by the side bathymetry and slowed down to a nearly constant value after approximately 300 s. The relative dispersion with t = 1 – 1000 s showed good fit (R^2 > 0.95) using power law relation with powers between 1 – 2 and exponential curves. However, transitions between regimes were likely distorted in the averaging approach adopted for the relative dispersion analysis. Thus FLSE is employed in examining the observable regimes.

In the scale of 10 – 30 m, the FSLE, $\lambda(\delta)$ log-log curves had a slope of -1 suggesting the existence of ballistic regimes. For the HR drifter dataset, the FSLE switched to a slope ~ -2/3 for spatial scale, δ ~ 2 – 10 m suggesting an existence of Richardson's power law regime. However in a similar spatial scale range, the LR showed an approximately flat $\lambda(\delta)$ spectrum corresponding to an exponential growth which is indicative of chaotic advection. The difference between the regimes displayed by two drifter types was likely related to the difference in inertial effect caused by difference in the physical size of the drifters. This could however not be confirmed because of the relatively small DOF in the FSLE estimate (see Figure captions). At a smaller scale, δ < 1 m, the LR drifter dataset indicated a power ~ -1. This was likely linked with ballistic behaviour of position uncertainty because the resolvable scale for the LR drifter was in the order of 1 m [12].

Figure 6 shows plots of relative dispersion, $D_p^2(t)$ and the FSLE , $\lambda(\delta)$ for cluster of HR and LR drifters deployed during EJ15 field experiment. During this experiment, the length of deployments, i.e. the length of pair-particle realisations varied between 81 and 3961 s. The dispersion was larger in the streamwise direction than in the cross stream direction indicative of anisotropic dispersion. The LR drifter formed an approximately circular patch after elapse time of 10 s before the spreading in the streamwise became significant. The $\lambda(\delta)$ curve showed an approximately flat FLSE spectrum corresponding to an exponential growth which is indicative of chaotic advection in the spatial scale of 0.4 – 10 m and 1 – 50 m for the HR and LR

drifter datasets, respectively. Power of -1 in the $\lambda(\delta)$ curves at smaller scales could be linked with ballistic behaviour of position uncertainty. Spatial scales δ > 50 m were not examined due to restriction in the length of deployment within the channel.

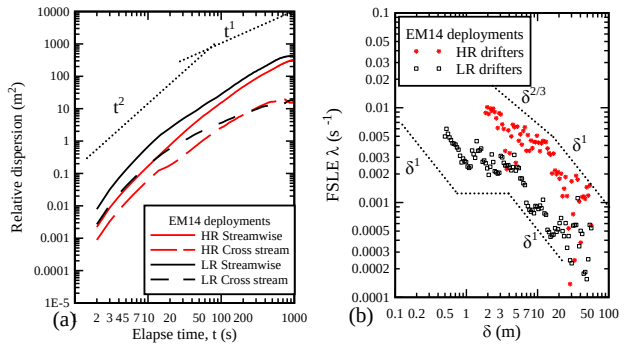

Figure 5. EM14 datasets (a) Relative dispersion as a function of elapsed time, t estimated from ensemble of 241 and 954 non-independent realisations for high (HR) and resolution (LR) drifter datasets, respectively; dash lines indicate power law scaling; (b) Finite scale Lyapunov exponents estimated from all possible realisations. Each data point consists of 6 - 12 (mean = 5.3) and 9 – 84 (mean = 45.8) realisations for HR and LR drifters, respectively.

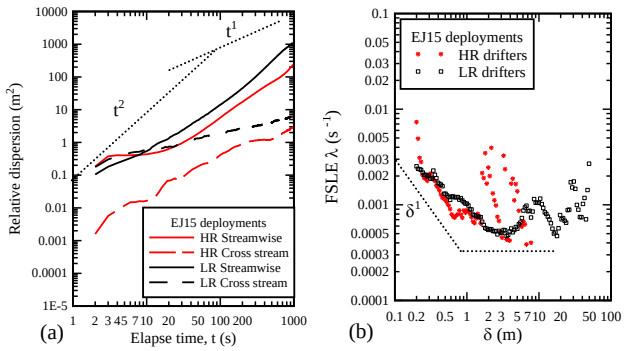

Figure 6. EJ15 datasets (a) Relative dispersion as a function of elapsed time, t estimated from ensemble of 590 and 1720 non-independent realisations for high (HR) and (LR) drifter datasets, respectively; dash lines indicate power law scaling; (b) Finite scale Lyapunov exponents estimated from all possible realisations. Each data point consists of 6 - 235 (mean = 76) and 6 – 258 (mean = 126) realisations for HR and LR drifters, respectively.

The FSLE analysis indicated the existence of exponential dispersive behavior at relatively large scale. The difference in the dispersion regimes observed between the two experiments was results of different Eulerian flow fields for example, tidal difference, bathymetry difference in the area studied and other environmental conditions. The FSLE estimates showed that dispersion during the EM14, neap tide experiment was a result combination of chaotic advection and turbulence within the resolved scale while behavior observed during EJ15, spring tide experiment was predominated by chaotic advection.

The relative dispersion from both field experiments showed that $D_p^2(t)$ scales as time, t in a Richardson-like relation with power between 1 – 2. The dispersion within the channel was generally weaker than Richardson's power law of 3 Nevertheless, diffusivities at small scale O (1 m) follow a 4/3 power law with length scale consistent with Richardson 4/3 scaling [9]. This suggests complex dispersion resulting from superposition of periodic modes in the underlying Eulerian field at the time scale range under study.

Summary and conclusion

Data from multiple deployments of low and high resolution clusters of GPS-drifters sampled at 1 Hz were used to examine mixing and dispersion behaviour of a small tidal estuary. The result showed that relative dispersion within the channel was generally weaker than Richardson's power law exponent of 3 with a power exponent in the range of 1 – 2. A relation, $\lambda \sim \delta^{-2/3}$ in the FLSE curve corresponding to Richardson's scale was observed at small scale, $\delta \sim 2 – 10$ m which implied the presence of turbulent mixing generated by the channel boundaries**.** The FSLE analysis suggested the presence of exponential dispersive behavior associated with chaotic advection at medium to large spatial scales. The difference in the dispersion regimes observed between the two experiments was likely the result of different Eulerian flow fields, for example tidal difference, bathymetry difference in the area studied and other environmental conditions.

Acknowledgement

The authors thank all people (QUT and UQ undergraduate students and staff) who participated in the field studies. The project is supported through ARC Linkage grant LP150101172.

References

[1] Richardson, L.F., Atmospheric diffusion shown on a distance-neighbour graph. *Proceedings of the Royal Society of London. Series A, Containing Papers of a Mathematical and Physical Character*, 1926. 110(756): p. 709-737.

[2] Sawford, B., Turbulent relative dispersion. *Annual review of fluid mechanics*, 2001. 33(1): p. 289-317.

[3] LaCasce, J., Lagrangian statistics from oceanic and atmospheric observations, in *Transport and Mixing in Geophysical Flows*. 2008, Springer. p. 165-218.

[4] Kolmogorov, A.N., Dissipation of Energy in the Locally Isotropic Turbulence. *Doklady Akad. Nauk SSSR 32, 141 (English translation 1991). Proceedings: Mathematical and Physical Sciences*, 1941. 434(1890): p. 15-17.

[5] Batchelor, G.K. Diffusion in a field of homogeneous turbulence. in *Mathematical Proceedings of the Cambridge Philosophical Society*. 1952. Cambridge Univ Press.

[6] LaCasce, J.& Bower, A., Relative dispersion in the subsurface North Atlantic. *Journal of marine research*, 2000. 58(6): p. 863-894.

[7] Spydell, M., Feddersen, F., Guza, R., & Schmidt, W., Observing surf-zone dispersion with drifters. *Journal of Physical Oceanography*, 2007. 37(12): p. 2920-2939.

[8] Brown, J., MacMahan, J., Reniers, A., & Thornton, E., Surf zone diffusivity on a rip-channeled beach. *Journal of Geophysical Research: Oceans*, 2009. 114(C11).

[9] Suara, K.A., Brown, R.J., & Borgas, M., Eddy diffusivity: a single dispersion analysis of high resolution drifters in a tidal shallow estuary. *Environmental Fluid Mechanics*, 2016: p. 1-21. doi: 10.1007/s10652-016-9458-z

[10] Suara, K.A., Wang, C., Feng, Y., Brown, R.J., Chanson, H., & Borgas, M., High Resolution GNSS-Tracked Drifter for Studying Surface Dispersion in Shallow Water. *Journal of Atmospheric and Oceanic Technology*, 2015. 32(3): p. 579-590.

[11] Lumpkin, R.& Elipot, S., Surface drifter pair spreading in the North Atlantic. *Journal of Geophysical Research: Oceans*, 2010. 115(C12).

[12] Haza, A.C., Özgökmen, T.M., Griffa, A., Poje, A.C., & Lelong, M.-P., How Does Drifter Position Uncertainty Affect Ocean Dispersion Estimates? *Journal of Atmospheric and Oceanic Technology*, 2014. 31(12): p. 2809-2828.